Towards Gbps Downlinks from Low-Cost Active Phased Arrays

Adam Gannon†, James Downey, Bryan Schoenholz
Communications & Intelligent Systems Division, NASA Glenn Research Center
Cleveland, Ohio, USA
†adam.gannon@nasa.gov

***Abstract*—Spacecraft performing science missions use high-directivity antennas to quickly downlink large amounts of collected data. Movement required to keep gimbaled reflector antennas trained on target receivers can impart blockages or vibrations which perturb precision science instruments. Recent manufacturing advances have made Ka-band electronically-steered antenna arrays a cost-effective option to mitigate these challenges, but only if these devices can be proven to deliver comparable quality of service. In this work we present a hardware and software architecture for high-rate links using an active phased array-based terminal in a 1U (10cm cube) form factor. Over-the-air tests in an antenna range characterize two key features of the architecture: high-order (32APSK and above) modulations and dual carriers. We calculate an optimal modulation-dependent input power backoff from array saturation and perform orbital simulations of the link at this operating point. We conclude that reliable links with rates in excess of 1Gbps are possible with current-generation hardware.**

***Index Terms*—active phased array antennas, 5G technology, small satellites, space communications, SKOUT, Nightingale**

I. Introduction

Space missions using high-precision instruments for collection of scientific data require highly stable platforms. Gimbaled reflector antennas offer high directivity but impart vibrations due to slewing movements as they track a receiving ground station. Fixed reflectors popular on small satellite platforms frequently require body pointing during communications which misaligns instruments with their observation targets. A large percentage of missions aim to continuously gather data over 100% of their orbits, making breaks in observation for communications detrimental. Active phased array (APA) antennas are an attractive option for high-directivity terminals which perform steering electronically with no moving parts. Additionally APAs offer advanced operations not possible with gimbaled reflectors including reduced slew times, formation of multiple spatial beams for simultaneous communication, beam shaping for interference prevention, and beam spoiling for reception under imperfect position knowledge. However product development timelines and per-unit costs have hindered adoption of APAs for space missions.

The availability of beamforming and frequency converter chipsets at commercial timelines and mass production volumes has greatly increased through the adoption of Fifth Generation (5G) mobile broadband technologies. Of particular interest is the n258 band (24.25-27.5GHz) which overlaps with Ka-band spectrum utilized for space-Earth links. Terminals based around these chipsets have the potential to offer Ka-band APAs for space missions at greatly reduced cost. However, these terminals must be proven to have capabilities matching that of traditional terminals to demonstrate their use to the science mission community. In this work we propose an architecture capable of closing Gbps-class downlinks from low-Earth orbit while requiring no mechanical motion onboard the spacecraft. Laboratory tests on an engineering model of the terminal are used to characterize operating points and predict performance.

This manuscript is a work of the United States Government authored as part of the official duties of employee(s) of the National Aeronautics and Space Administration. No copyright is claimed in the United States under Title 17, U.S. Code. All other rights are reserved by the United States Government. Any publisher accepting this manuscript for publication acknowledges that the United States Government retains a non-exclusive, irrevocable, worldwide license to prepare derivative works, publish, or reproduce the published form of this manuscript, or allow others to do so, for United States government purposes.

II. Hardware & Software Design

The hardware used for these experiments is the CesiumAstro Nightingale terminal [1] which consists of a 186-element APA paired with credit card-sized modules: an up/down converter (UDC), power conditioning unit (PCU), single-board computer (SBC), and software-defined radio (SDR). Fig. 1 outlines the test setup in a portable antenna range [2] with the array mounted in a thermal control system [3] to operate at a +20°C set point. While the APA and UDC have an instantaneous bandwidth of 1GHz, the two independently-tunable channels of the SDR produce narrower bandwidths. The SDR uses

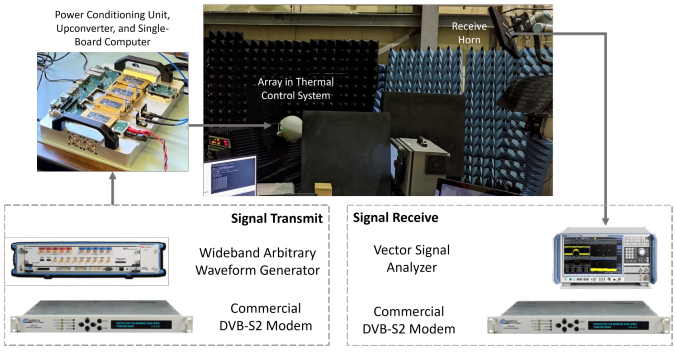


Fig. 1. APA and related hardware test setup in antenna range.

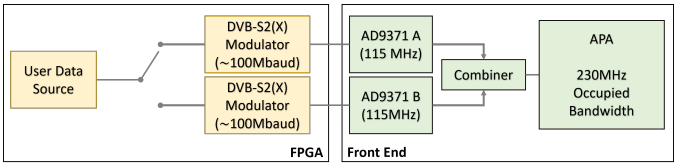


Fig. 2. Diagram of proposed dual-channel transmitter design.

the AD9371 transceiver [4] which can synthesize 250MHz per-channel of which 100MHz is well-characterized, large-signal bandwidth. Significantly wider bandwidths begin to be affected by a decrease in linearity. Similar to [5] we propose a digital design, implemented on the SDR's field programmable gate array (FPGA), which utilizes two independent modulators following the 2nd Generation Digital Video Broadcast – Satellite standard (DVB-S2) and its extensions (DVB-S2X) [6]. Each modulator operates at 100Mbaud and pulse shapes with a 15% root-raised cosine filter. Simulations with Analog Devices software indicate reasonable performance of these 115MHz signals through the SDR's transceiver chips. As in Fig. 2, output from each modulator is tuned with a small frequency offset and combined in analog to form a dual-channel composite signal. To reduce risk for a full FPGA implementation we use a Keysight M8190A arbitrary waveform generator as a signal source for this work. A high-stability oscillator is distributed to each instrument as a frequency reference.

III. Optimal Operating Point

A. Backoff Determination

Peak-to-average power ratio (PAPR) influences the amount of input power backoff needed to maintain a given level of linearity as a signal is passed through a power amplifier. PAPR is a statistical quantity usually described as dB above average power at 1% probability in a complementary cumulative distribution function. As shown in Fig. 3, the quantity is modulation dependent with the PAPR of 256APSK signals approximately 1.2dB greater than that of QPSK.

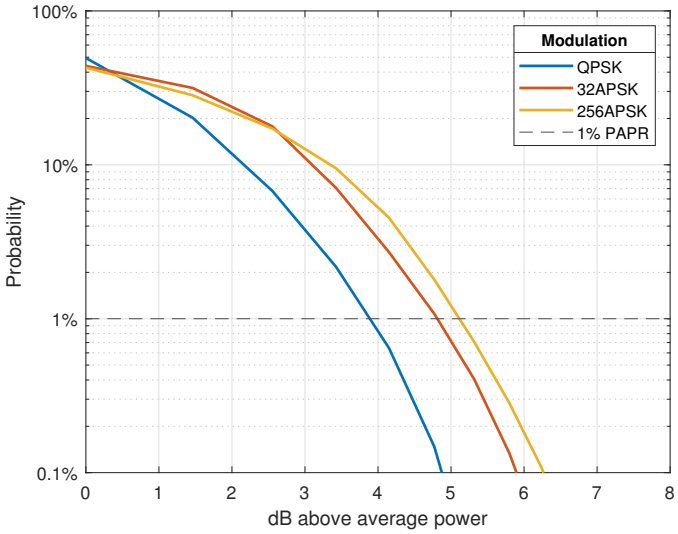


Fig. 3. Calculated PAPR of single signal across simulated samples of various modulations with a 15% root-raised cosine filter applied.

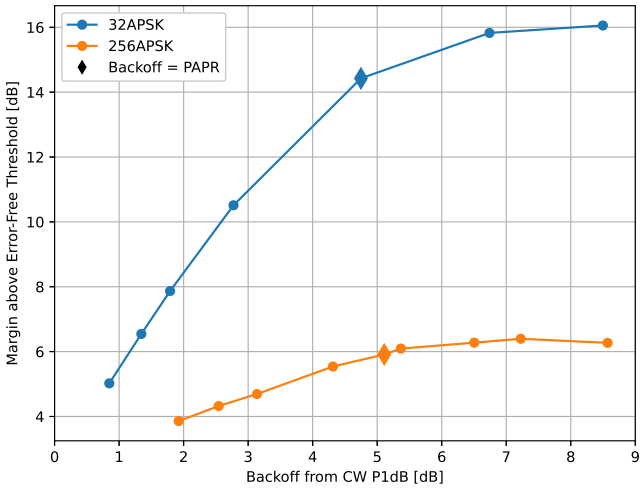


Fig. 4. Measured margin above QEF threshold as a function of backoff from P_{1dB} for two modulations. Diamonds indicate backoff equal to PAPR.

The waveform generator was used to source each modulation type through the array and a Rohde & Schwarz FSW vector signal analyzer (VSA) coupled to the receive horn measured modulation error ratio (MER). The effective isotropic radiated power (EIRP) of the array was varied relative to the measured 1dB compression point (P_{1dB}) of a continuous wave signal (60.5dBm at 20°C). MER, which approximates E_S/N_0 over sufficiently long measurement windows, was compared against the quasi error free (QEF) thresholds in the DVB-S2(X) standards to yield margin shown in Fig. 4. We note this is a rough comparison since thresholds in the standards assume only white Gaussian noise and not the non-linear effects of amplifiers. To gain confidence in this metric as an approximation of performance, a Comtech CDM-760 DVB-S2X modem was connected to each side and frame error rate metrics taken at the maximum tested EIRP of each modulation. As expected with a ∼4dB margin, zero frame errors were recorded by the modem over 1e6 frames. From Fig. 4 we observe that the optimal operating point appears to be when backoff[1] is equal to PAPR. This operating point is at the bend of each curve — the highest output power before margin begins to steeply decline.

B. Dual Modulators

As is a known issue in multi-carrier transmissions, the addition of output from a second independent modulator will increase PAPR of the combined signal. Simulations show an increase of 0.8-1.0dB (Table I). To verify this effect, samples generated by a second independent modulator were output on the waveform generator's second channel and combined in the

[1]Operating at these points puts us in the linear region of the APA where input power backoff and output power backoff are almost exactly equal. We will simply use "backoff" in the remaining text.

UDC. MER of the first signal was measured with the second signal spaced far away yet still in the operating bandwidth of the APA. A corresponding MER increase of 2.5dB was measured. As in Fig. 5, an additional backoff approximately equal (within gain control granularity) to the PAPR increase is necessary to return MER of the combined signal to the optimal operating point.

Frequency offset between the two signals was adjusted to determine optimal separation. Spacing between carriers at least equal to the signal bandwidth produced no noticeable degradation in MER in excess of the 2.5dB already noted above. At this spacing, the necessary bandwidth [7] of the signal is 230MHz. That is, a receiver operating over 230MHz of bandwidth at 27GHz should be able to demodulate both independent signals centered at 26.9425GHz and 27.0575GHz. Depending on receiver architecture it may be necessary to include an analog filter to separate the signals. In range experiments the filtering in the VSA itself was sufficient.

Modulation	Single (dB)	Dual (dB)
32APSK	4.8	5.8
256APSK	5.2	6.0

TABLE I
CALCULATED BACKOFF POINTS FOR SINGLE AND DUAL TRANSMITTERS.

IV. Orbit Prediction

We use an orbital mechanics and link analysis tool [8] to predict performance from a spacecraft in 550km sun-synchronous orbit (a popular choice for small satellite missions). The antenna is nadir-facing and electronically steers within an off-boresight angle θ of $\pm 60°$. We apply the backoffs in Table I to the nominal EIRP of the APA. EIRP is further reduced by scan loss equal to $10\log(\cos^x\theta)$ dB with $x = 1.31$ characterized from near field measurements of the array. NASA's 11m ground station at Wallops Island, Virginia (WG5) is assumed for the receiver. Received E_S/N_0 for each signal was simulated considering path loss corresponding to a center frequency of 27GHz and limited to maximum values due to amplifier distortion as measured in Fig. 4.

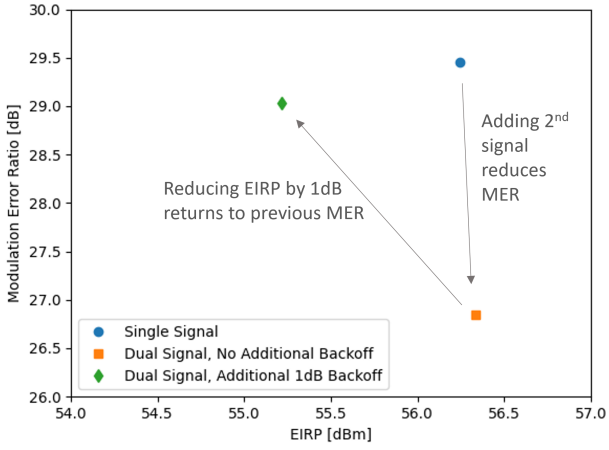


Fig. 5. Effect on measured MER for 32APSK as a second signal is added and then additional backoff equal to the calculated PAPR increase is applied.

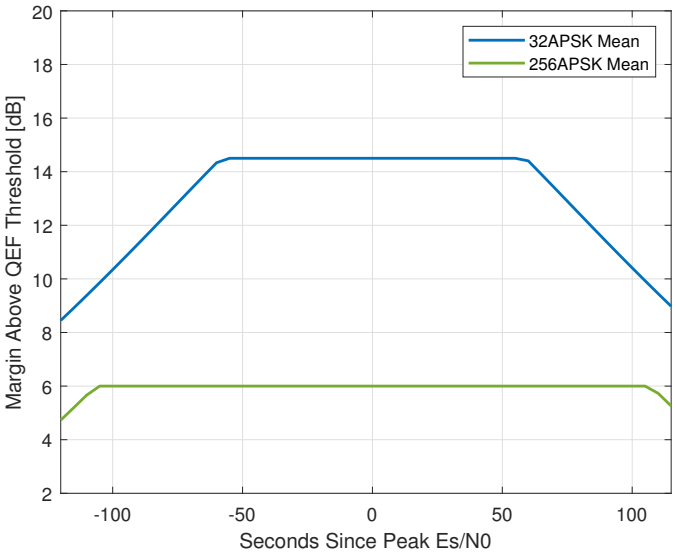


Fig. 6. Simulated margin above QEF threshold during passes from LEO to WG5 for 32 and 256APSK. Average taken over three months.

Calculations were run for a simulated three months totaling 166 passes of at least 4 minutes. Comparison against the QEF thresholds in the standards yields the margins shown in Fig. 6. We observe that even with the applied backoff there remains plenty of margin throughout the pass. From rates[2] in Table II, the dual modulator approach results in data transfer of 25GB per pass at the maximum rate modulation/coding in the DVB-S2 standard (32APSK 9/10) and 33GB at the maximum of the DVB-S2X standard (256APSK 3/4).

Modulation/Coding	Num. Modulators	User Rate (Mbps)
32APSK 9/10	1	450
	2	900
256APSK 3/4	1	600
	2	1200

TABLE II
ACHIEVABLE USER RATE FROM LEO AT 100MBAUD.

V. Conclusion

In summary, use of high-order modulations with APAs is feasible particularly in bandwidth-limited cases where additional backoff from P_{1dB} can be applied while still maintaining positive link margin. In antenna range tests with a representative APA, we demonstrated a dual-modulator design is also practical provided the increase in PAPR due to addition of a second signal is accounted for. Even when paired with an SDR with per-channel bandwidths narrower than the instantaneous bandwidth of the APA, rates in excess of 1Gbps are achievable.

[2]Overhead will reduce the user information rate by approximately 1-5% from these raw bitrates based on choice of frame size and inclusion of pilots.

Data rates in this range are competitive with reflector antenna and tube amplifier architectures used in traditional Ka-band transceivers while occupying significantly less mass and volume. For example, the 1.2Gbps calculated above is equal to the downlink rate of the Plankton, Aerosol, Cloud and Ocean Ecosystem (PACE) mission and approaches the 1.75Gbps per-polarization rate of the NASA-ISRO Synthetic Aperture Radar (NISAR) mission [9]. Critically, this data transfer would take place with no motion required by or imparted on the spacecraft. This design, based on hardware currently commercially available, provides flexibility to continue observations during communications cycles provided the spacecraft power budget can support such simultaneous operation.

VI. Acknowledgments

We thank Phil Paulsen for his helpful insight on APA mission use cases. This work was performed under the SmallSat Ka-band Operations User Terminal (SKOUT) project, funded by NASA's Space Communications and Navigation program.

References

[1] S. Sabripour, J. Haque, A. Ciszmar, and T. Magesacher, "A COTS-based software-defined communication system platform and applications in LEO," in *36th International Communications Satellite Systems Conference (ICSSC)*, Niagara Falls, Canada, Oct 2018.

[2] P. A. Slater, J. M. Downey, M. T. Piasecki, and B. L. Schoenholz, "Portable laser guided robotic metrology system," in *2019 Antenna Measurement Techniques Association Symposium (AMTA)*, Minneapolis, MN, Nov 2019.

[3] B. L. Schoenholz, J. M. Downey, and M. T. Piasecki, "Design of a thermal testbed for metrology of active antennas," in *2022 Antenna Measurement Techniques Association Symposium (AMTA)*, Denver, CO, Oct 2022.

[4] N. Franconi, S. Sabogal, A. George, M. Hassouneh, J. Mitchell, and C. Wilson, "A novel rf architecture for simultaneous communication, navigation, and remote sensing with software-defined radio," in *34th Annual AIAA/USU Conference on Small Satllites (SmallSat)*, Logan, UT, Aug 2020.

[5] K. Devaraj, M. Ligona, E. Blossom, J. Breu, B. Klofas, K. Colton, and R. Kingsbury, "Planet high speed radio: Crossing gbps from a 3u cubesat," in *33rd Annual AIAA/USU Conference on Small Satllites (SmallSat)*, Logan, UT, Aug 2019.

[6] "Digital video broadcasting (DVB) second generation part 2: DVB-S2 extensions (DVB-S2X)," European Telecommunications Standards Institute (ETSI), Standard ETSI EN 302 307 v1.2.1, May 2020.

[7] "Manual of regulations and procedures for federal radio frequency management, annex j: Guidance for determination of necessary bandwidth," National Telecommunications and Information Administration (NTIA), Standard, Jan 2022.

[8] J. M. Shah and B. W. Welch, "Space communications and navigation (SCaN) tool capabilities updates for antenna pattern and jitter," NASA Glenn Research Center, Tech. Rep. NASA/TM—2019-220233, 2019.

[9] P. Baldwin, V. Anderson, R. W. Chang, A. Svitak, T. William, S. El-Nimr, D. Kaul, M. Perrine, and K. Abhyanka, "Nasa 26 ghz polar subnet in 2020+," in *15th International Conference on Space Operations (SpaceOps)*, Marseille, France, May 2018.